

# FEMTOSECOND STABLE LASER-TO-RF PHASE DETECTION FOR OPTICAL SYNCHRONIZATION SYSTEMS

T. Lamb\*, M. K. Czwalinna, M. Felber, Ch. Gerth, H. Schlarb, S. Schulz, C. Sydlo, M. Titberidze, F. Zummack, DESY, Hamburg, Germany,  
Ewa Janas, Warsaw University of Technology, Warsaw, Poland,  
Jaroslaw Szewinski, National Centre for Nuclear Research (NCBJ), Swierk, Otwock, Poland

## Abstract

Optical reference distributions have become an indispensable asset for femtosecond precision synchronization of free-electron lasers. At FLASH and for the future European XFEL, laser pulses are distributed over large distances in round-trip time stabilized fibers to all critical facility sub-systems. Novel Laser-to-RF phase detectors will be used to provide ultra phase stable and long-term drift free microwave signals for the accelerator RF controls. In this paper, we present the recent progress on the design of a fully integrated and engineered version of the L2RF phase detector, together with first experimental results demonstrating so-far unrivaled performance.

## INTRODUCTION

Tight locking of microwave signals to an optical pulse train from a mode-locked laser can be performed in different ways. A photo diode in conjunction with a narrow band-pass filter at a laser harmonic and mixing to baseband is the standard and most straight forward method. However, to overcome photo diode drifts and excess noise more elaborate arrangements using a balanced Sagnac loop interferometer where proposed and successfully demonstrated at a rather high radio frequency (RF) of 10.2 GHz [1]. Our proposed technique is also well suited for lower frequencies, e.g. the 1.3 GHz accelerating frequency at FLASH, where the time-to-phase conversion constant is proportionally smaller. Femtosecond stability at lower RF frequencies therefore requires a significantly improved phase detector sensitivity of the laser-to-RF (L2RF) converter and by careful engineering ultra-low drift characteristics have to be ensured.

The L2RF phase detector output is fed to a phase-look-loop (PLL) for either locking a low noise RF source to the laser reference, or vice versa, to lock laser oscillator to an RF reference e.g. to overcome the pure noise behavior of mode-locked lasers at low offset frequencies. For FLASH and the European XFEL, 1.3 GHz RF reference will be distributed through coaxial cables providing low phase noise microwave characteristics, but the RF signal will be subjected to drifts in the 100 fs range [2]. Here, the L2RF setup will be used in the optical reference module (REFM-OPT) to remove low offset phase noise and drifts using a simple phase shifter for corrections. Further details on the optical and RF synchronization system can be found in [3, 4, 5].

\*Thorsten.Lamb@desy.de

## LASER-TO-RF SETUP

The heart of the L2RF setup is a commercially available Mach-Zehnder amplitude modulator (MZI) where the ultra-short laser pulses with sub-picosecond duration sample the amplitude of the RF. No laser pulse modulation is observed if the optical pulses hit the zero-crossing of the RF wave. To distinguish MZI bias-offset drifts or laser power variations from phase changes of the RF, the laser pulse train is split and recombined such that the laser pulses now sample the positive and negative zero crossings of the RF wave. Phase errors now impose a (sub-)harmonic amplitude modulation onto the recombined laser pulse train which is filtered, strongly amplified and readout by a synchronous detection circuit with high precision. Further details of the operation principle of the L2RF phase detector can be found in [6].

### Engineered Opto-Mechanics

The opto-mechanics for the free-space split, delay and recombination of the laser pulses is shown in Fig. 1. It consists of a solid aluminum base-plate with cutouts for the various optical components. The laser beam exiting the input collimator (in), passes optionally motorized  $\lambda/2$  and  $\lambda/4$  waveplates (L/2 and L/4) for polarization control. A small fraction of the optical power is tapped to generate the local oscillator (LO) signal required for the synchronous detection electronics. The optical beam is then split and recombined by a polarizing beam cube where the first delay length can be adjusted with high precision. A cleanup polarizer and  $\lambda/2$  waveplate are used to adjust the polarization launched into the polarization maintaining input fiber of the MZI.

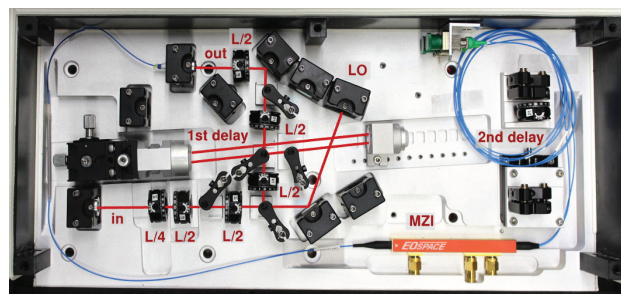


Figure 1: Engineered Opto-mechanical setup.

The MZI is mounted at the corner of the aluminum base plate in order to minimize the cable length to the MZI-RF-input. The selected MZI has an RF output port permitting

higher RF power transmission before thermal destruction. The MZI bias voltage for balanced transmission can be provided by the central SMA connector. The selected MZI features two output ports ( $b$ ,  $\bar{b}$ ). If both ports are recombined by a certain delay (second adjustable delay) the sensitivity of the setup can be further improved and the susceptibility to mechanical movements causing pulse train amplitude imbalances of the recombined pulse train in the first delay line be removed (see [6]).

The humidity and temperature stability of the optical setup is crucial for the L2RF performance. Thus careful engineering was conducted and experimentally verified. On top of the base plate sits a housing of high density polyethylene (HD-PE). The housing seals the box from humidity changes and it is supporting the thermal insulation of the box. The different elements of the housing are glued together in order to seal the joints, the flexible connections include rubber gaskets. The RF-feed-throughs are sealed with o-ring gaskets, while in- and outgoing fibers are guided through the cover's gaskets in a special area.

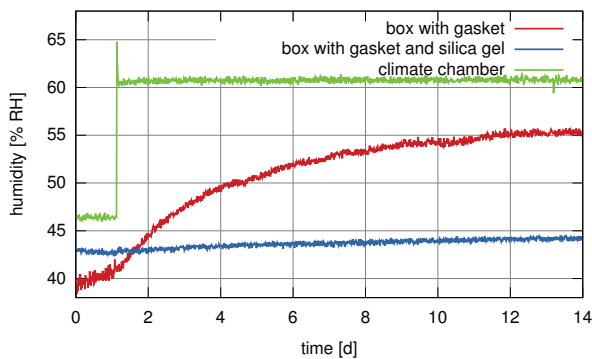


Figure 2: Humidity stability of the L2RF base plate.

The sealed box limits air transfer into and out of the housing, but humidity changes still slowly affect the inner conditions. For further stabilization a dust-proof sachet filled with 250 g of a special silica gel called *pro sorb* [7] is mounted inside the housing. This sachet buffers the remaining humidity variations. At 50% RH *pro sorb* can store about 30% of water relative to its own weight. This is higher than the capability of standard silica gel at this relative humidity. Measurements of two closed housings (one without silica gel) in a climate chamber reveal, that this humidity

stabilization works very well (see Fig. 2). For a sudden change of 15 % RH, the box with silica gel follows only about 2.3 % RH peak to peak within almost two weeks. The box without silica gel, which was only passively sealed, followed in the same time with a full 15 % RH change.

The temperature stabilization was also tested in a climate chamber. The aluminum base plate is mounted with two peltier elements onto a heatsink. The Peltier elements can cover a maximum of 30 W thermal load each. Both Peltier elements are connected in series to one analogue temperature controller (Team Wavelength PTC10k-CH) and the loop sensor was placed close to the MZI on top of the base plate. The measurement reveals, that due to thermal losses through the outer insulation (9 mm thick elastomeric thermal foam,  $0.035 \text{ W/Km}$ ) and finite thermal conductivity of the base plate (aluminum,  $235 \text{ W/Km}$ ), a temperature gradient is formed over the base plate. Additionally, this gradient slightly changes with the outer temperature and in this way limits the performance of the temperature control. The test was performed with a temperature step of  $30 \text{ }^\circ\text{C}$ . At the MZI, a temperature variation of 0.3 K has been detected, while in a the base plate corner next to the sensor 1.4 K and in the farthest corner 3.1 K have been measured. For different positions of the base plate one can now calculate suppression factors between 100 and 10. The expected temperature stability in the low-level RF (LLRF) racks in the accelerator is  $\pm 1 \text{ K}$ , which leads to the conclusion that the achievable temperature stability will be between 0.1 K and 0.01 K.

To further improve the temperature stability, one could increase the thickness of the outer insulation to reduce the temperature gradient over the plate, but this is difficult due to space constraints in the 3 HU 19" box, the optics have to fit in later. Alternatively one could use a second temperature controller. Regulating both Peltier elements individually will minimize the gradient over the base plate and therefore also the sensitivity to variations of the outer temperature.

### Engineered Electronics

The detector electronics have been integrated into a single printed circuit board (PCB) within a custom housing. This provides significant advance over the original setup, which was composed of dedicated RF components, large manual phase shifters and various cable connections. The compact, integrated readout electronics is now well suited for an accelerator environment.

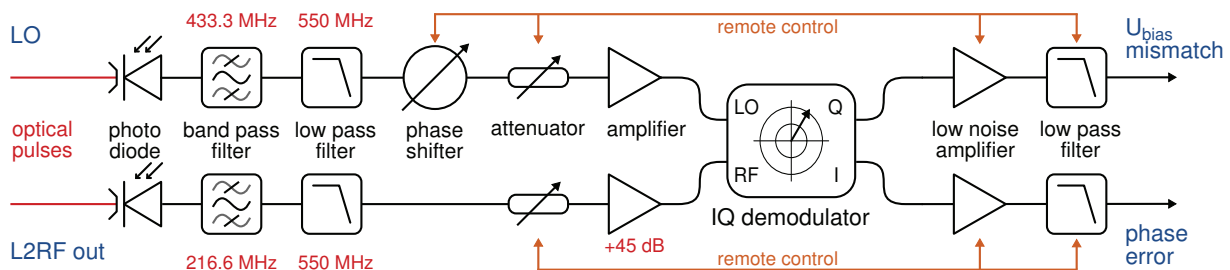


Figure 3: Simplified block diagram of the L2RF readout PCB.

The board has internal PT1000 sensors for temperature monitoring. RF-gains are remote selectable, as well as gain and bandwidth of the low noise output amplifiers after the demodulator. The internal LO phase is remote controllable with on-board electronic phase shifters (see Fig. 3). The board has three main output signals which can all be used to set up feedback loops on dedicated parameters. The most important output signal is the phase signal which drives the actual PLL. Additionally, bias drifts of the MZI are detected and the bias voltage of the MZI is continuously stabilized. The third output detects drifts of the first optical delay line. He is only monitored, In a later revision it would also be possible to actively stabilize this optical delay line if needed.

The digital interface for remote control is right now connected to the first prototype of a general purpose FPGA based controller board (TMCB), which is meant to be used in many LLRF units for the European XFEL. The board will be replaced with a second revision and is also meant to perform monitoring and temperature control tasks in the future. Additionally, the board will also take care of the actual PLL. As the TMCB will be the only digital controller involved, it is easily possible to integrate the whole L2RF setup for later usage in the accelerator.

### Humidity Influence on RF-Cables

To enable drift measurements with femtosecond precision over long time periods special care on the interconnecting RF cables has to be taken. Measurements in a climate chamber revealed, that even so called ultra phase stable RF cables suffer from a significant humidity dependence. We found a  $\frac{1}{e}$  time constant of typically ten to twenty hours influencing our precise phase drift measurements. Thus proper cable selection and environmental control turned out to be crucial. The humidity coefficients of different coaxial cables have been determined by applying a large humidity step in a climate chamber while recording the phase change of the cables. The phase changes were detected using AD8302 based phase detectors and an Agilent 34970A data acquisition unit. The measurements were carried out at 1.3 GHz at a temperature of 25 °C. The measurement results are presented in Table 1, including cable temperature coefficients at 25 °C. While most laser rooms are meanwhile temperature stabilized to  $\pm 0.1$  K or better, for precision synchronization systems humidity control turns out to be even more important.

Table 1: RF Cable Properties

cable type	$f_s/\%RH_m$	$f_s/K_m$
<b>Pasternack [8]</b>		
PE-SR402FL	9.6	-183
<b>Huber &amp; Suhner [9]</b>		
Sucoflex 404	3.5	26
<b>Teledyne Storm Microwave [10]</b>		
Phasemaster 190-874	3.4	15

## PERFORMANCE MEASUREMENTS

The achievable short-term accuracy of the L2RF phase detector is limited by the noise floor of the photo diodes and read-out electronics. In Figure 4 the output noise within a bandwidth of 1 Hz to 10 MHz is plotted for different gains of the switchable low-noise output amplifier and without RF connected. The lower plot shows the integrated noise, converted to femtoseconds using separately at 1.3 GHz obtained calibration constants (see Table 2). In the upper part of this plot, the decade wise integrals are given.

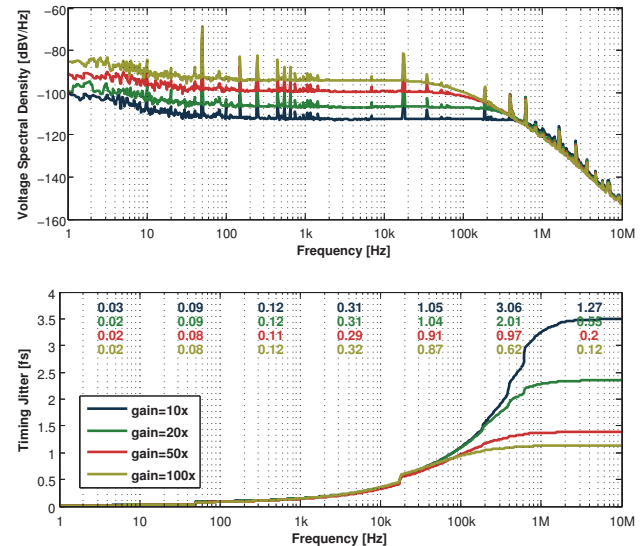


Figure 4: Detection limit of the L2RF detector.

For the highest gain setting of 100, the noise over the full bandwidth amounts to only 1.1 fs, while for frequencies up to 50 kHz all curves accumulate about 0.8 fs noise floor.

Table 2: L2RF Calibration Constants

gain	10	20	50	100
$K_\phi$ [V/ps]	0.72	1.41	3.48	5.73

To evaluate the long-term performance two L2RF phase detectors have been built. L2RF 1 was used to synchronize a low phase noise dielectric resonator oscillator (DRO) using an analog PPL. The RF output of L2RF 1 was connected to the RF input of L2RF 2 in order to perform an out-of-loop measurement (see Fig. 6).

The long-term measurement was conducted with a gain of 20. The two L2RF setups were connected with a 250 mm Phasemaster 190 cable. The  $K_\phi$  of the in-loop detector is 1.41 V/ps, while the out-of-loop detector showed a lower  $K_\phi$  of about 0.73 V/ps. The data was taken with an Agilent 34970A data acquisition unit, with a sample rate of 0.1 Hz. The measurement result is shown in Fig. 5.

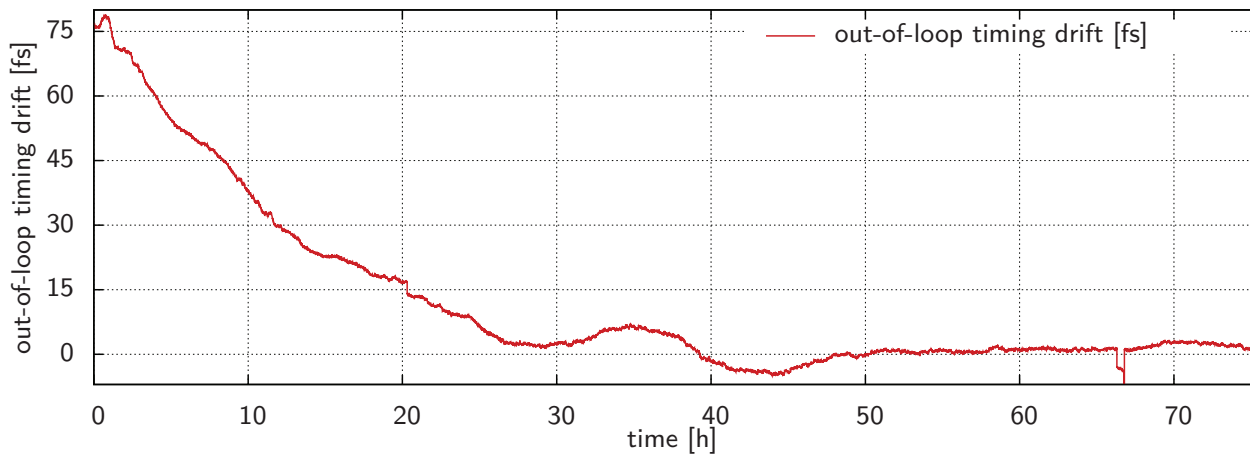


Figure 5: Out-of-loop timing of the L2RF drift measurement.

A first measurement was interrupted by a power cut after only a few hours. The power cut also affected the climate control unit and all the auxiliary electronics in the lab. The burn-in phase of roughly 24 h at the beginning of the presented measurement while conditions in the laboratory stabilize again is a result of this power cut.

module is in preparation as well as the second revision of the TMCB needed for control tasks. The REF-M-OPT for the European XFEL will consist of these components, integrated in a 3 HU 19” housing.

Two first prototypes will be assembled and tested at FLASH as soon as possible.

## REFERENCES

- [1] J. Kim, et al., “Drift-free femtosecond timing synchronization of remote optical and microwave sources”, *Nature Photonics* 2 (733 – 736), 2008. doi:10.1038/nphoton.2008.225
- [2] K. Czuba, et al., “Overview of the RF Synchronization System for the European XFEL”, *Proceedings of IPAC13, Shanghai, China, 2013, WEPME35*, <http://www.JACoW.org>
- [3] S. Schulz, et al., “Past, Present and Future Aspects of Laser-Based Synchronization at FLASH”, *Proceedings of IBIC13, Oxford, UK, (2013), WEP32*, <http://www.JACoW.org>
- [4] C. Sydlo, et al., “Development Status of Optical Synchronization for the XFEL”, *Proceedings of IBIC13, Oxford, UK, (2013), MOP32*, <http://www.JACoW.org>
- [5] J. Branlard, et al., “The European XFEL LLRF System” ,*Proceedings of IPAC12, New Orleans, USA, (2012), MOAC01* <http://www.JACoW.org>
- [6] T. Lamb, et al., “Femtosecond Stable Laser-to-RF Phase Detection Using Optical Modulators”, *Proceedings of FEL11, Shanghai, China, (2011), THPA32*, <http://www.JACoW.org>
- [7] C. Waller, Long life for art, product description, (2013), <http://www.cwaller.de/eprosorb.htm>
- [8] Pasternack, datasheet, (2013), <http://www.pasternack.com/images/ProductPDF/PE-SR402FL.pdf>
- [9] Huber & Suhner, datasheet, (2013), <http://www.huber-suhner.com/de/Recent-Products/SUCOFLEX-400>
- [10] Teledyne Storm Microwave, datasheet, (2013), [http://www.teledynestorm.com/pdf/Phase\\_Master\\_190E.pdf](http://www.teledynestorm.com/pdf/Phase_Master_190E.pdf)

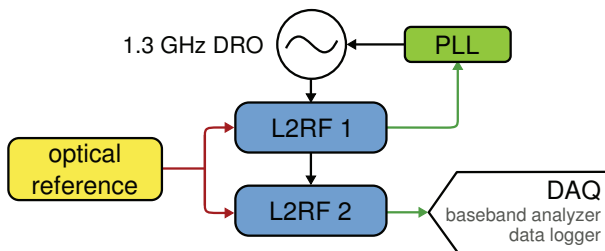


Figure 6: Long-term drift measurement setup.

The feature at 66.5 h measurement time was caused by an accidentally restarted server in the control system. After recovery, the measurement returned exactly to the same value as before the incident. Therefore this spike can be neglected.

The peak-to-peak stability finally amounts to only 12 fs for the last 48 h while the last **24 h show 3.6 fs peak-to-peak stability**.

At this moment, this performance for a 1.3 GHz laser-to-RF phase-locked loop is unmatched and the stability requirements of sub-10 fs for the complete chain including fiber link is reachable.

## SUMMARY & OUTLOOK

The stability of the laser-to-RF phase detector was demonstrated with 3.6 fs peak-to-peak over 24 h.

The opto-mechanical setup and the readout electronics have been successfully integrated and are ready for installation into the accelerator. The 1.3 GHz integrated control